Composites: Part B 44 (2013) 212–217

Contents lists available at SciVerse ScienceDirect

Composites: Part B

journal homepage: www.elsevier.com/locate/compositesb

Localized indentation of sandwich panels with metallic foam core: Analytical models for two types of indenters

Zhongyou Xie [a,b], Zhijun Zheng [a,*], Jilin Yu [a]

[a] CAS Key Laboratory of Mechanical Behavior and Design of Materials, University of Science and Technology of China, Hefei, Anhui 230026, PR China
[b] Department of Civil and Architectural Engineering, Tongling University, Tongling, Anhui 244000, PR China

ARTICLE INFO

Article history:
Received 7 January 2012
Accepted 29 May 2012
Available online 6 June 2012

Keywords:
A. Foams
A. Plates
C. Analytical modeling
Localized indentation

ABSTRACT

Sandwich structures with metallic foam core are sensitive to local indentation because of the low strength of the core and low bending stiffness of the thin face sheets. In this paper, local indentation response of sandwich panels with metallic foam core under a flat/spherical indenter was analyzed. The composite sandwich is modeled as an infinite, isotropic, plastic membrane on a rigid-plastic foundation. For simplicity, a quadratic polynomial displacement field was employed to describe the deformation of the upper face sheet. By using the principle of minimum work, explicit solutions for the indentation force and the sizes of the deformation regions were derived. The analytical results were verified by those from simulation by using the ABAQUS code, and they are in close agreement. Distribution of radial tensile strain of the upper face sheet and the ratio of energy dissipation of foam core to that of the upper face sheet were analyzed.

1. Introduction

Owing to the low strength of the core and low bending stiffness of the thin face sheets, sandwich structures with metallic foam core are prone to causing local indentation under concentrated loads such as handling, interaction with attached structures or impact. Researches have indicated that indentation behavior of sandwich panels with foam cores is mainly affected by some factors such as the foam core material, face sheet thickness and indenter size [1–4]. Some analytical models focused on elastic response of the whole sandwich structures [5–8], while some others studied the sandwich structures composed of elastic face sheets and plastic foam core [9,10]. The indentation response under a point or line load was examined in the analytical models of Refs. [7] and [10], whereas the influence of indenter size was introduced in the papers [5,6,8,9].

All of the solutions mentioned above are based on the assumption of elastic behavior of the top face sheet, and no one gives a clear description of the development of its plastic deformation. In general, sandwich structures with metallic face sheets and metallic foam core are prone to large indentation. Therefore, it is of great importance to obtain concise solutions of plastic response of the top face sheet. On the other hand, the typical compressive stress–strain curve of metallic foams has a plateau that the stress keeps almost constant in a large range of strain, so the foam core can be modeled as an ideally plastic foundation with a constant crushing resistance.

In this paper, the plastic indentation response of foam core sandwich circular panels dented by a rigid indenter with a finite radius was analyzed based on the principle of minimum potential energy. Solutions for the indentation force and deformation profile were derived. An FEA model was established by using the ABAQUS code to verify the validity and applicability of the analytical solutions.

2. Analytical modeling

Consider a sandwich circular panel with metallic foam indented by a rigid flat/spherical indenter, as shown in Fig. 1. The radiuses of the flat-end cylindrical indenter and the spherical indenter are both R. The circular panel has an infinite radius and consists of two face sheets and a foam core with thicknesses h and c, respectively. The flow stress of the face sheet material is σ_0. The foam core has a constant plateau stress σ_{pl}. There is an axisymmetic deformation region in the panel indented by an axisymmetic indenter. The indentation displacement of the indenter is denoted by δ, and the radius of the deformation region is denoted by ξ. The deformation field of the top face sheet in the loading direction is described by $w(r)$ with r being the radius.

The top face sheet of the composite structure can be considered as a fully clamped circular plate under transverse deflection, and radial displacements as well as circumferential membrane force may be neglected [11]. Additionally, plastic work due to shear force

* Corresponding author. Tel.: +86 551 360 3044; fax: +86 551 360 6459.
E-mail address: zjzheng@ustc.edu.cn (Z. Zheng).

1359-8368/$ - see front matter © 2012 Elsevier Ltd. All rights reserved.
http://dx.doi.org/10.1016/j.compositesb.2012.05.046

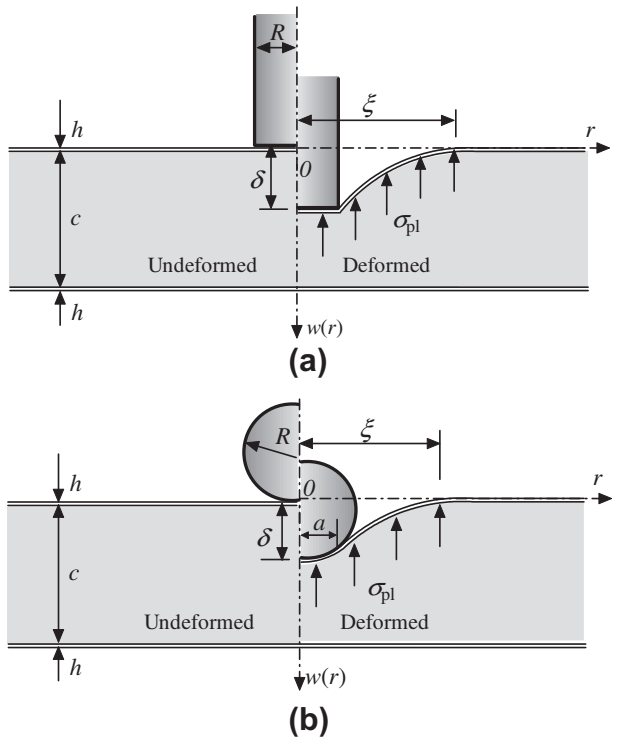

Fig. 1. Schematic profiles of undeformed and deformed zones of sandwich circular panels loading (a) under a flat indenter and (b) under a spherical indenter.

may be also neglected when the ratio of radius of the plate to its thickness exceeds 2 [12]. Hence, the plastic work of the top face sheet are mainly contributed by the radial bending moment M_r, the circumferential bending moment M_θ and the radial membrane N_r. Using the normality rule of the plasticity theory, Zaera et al. [13] have proposed a yield criterion

$$\left(\frac{N_r}{N_0}\right)^2+\left(\frac{M_r}{M_0}\right)^2+\left(\frac{M_\theta}{M_0}\right)^2-\frac{M_rM_\theta}{M_0^2}=1 \tag{1}$$

with $N_0=\sigma_0 h$ and $M_0=\sigma_0 h^2/4$ being the fully plastic membrane force and the bending moment of the face sheet, respectively. However, the influence of bending moment can be neglected when transverse displacement exceeds $h/2$. We focus on this case in this paper, so the top face sheet can be modeled as a plastic membrane on a rigid-plastic foundation.

Based on the principle of minimum potential energy, solutions for the indention response can be derived. The total potential energy of the system is

$$\prod = U+D-W \tag{2}$$

where U is the plastic strain energy of the top face sheet, D the plastic work due to compressive deformation of the foam core, and W the external work calculated by

$$W=\int_0^\delta P\mathrm{d}\delta \tag{3}$$

with P being the indentation force.

2.1. Under a flat indenter

A deformation field or a velocity field is generally assumed in such problems. Turk et al. [9] proposed a shape-function to describe the deformation of the upper face sheet to study the case of an infinite, orthotropic, elastic plate resting on a rigid-plastic foundation. In our previous study [14], we employed a linear velocity field to study the indentation response of sandwich beams, which leads to a closed-form deformation field in a quadratic polynomial function. For simplicity, we consider the indenter contacts closely to the top face sheet and the transverse displacement out of the contact region is described by a quadratic polynomial function with respect to the radial coordinate r, i.e.

$$w(r)=\begin{cases}\delta, & r\leqslant R\\ \delta\left(1-\frac{r-R}{\xi-R}\right)^2, & R<r\leqslant\xi\end{cases}. \tag{4}$$

When the radial membrane force is evaluated as the fully plastic value, the plastic work owing to the radial membrane can be calculated by

$$U=\int_A N_0\varepsilon_r\mathrm{d}A=\frac{\pi}{3}\sigma_0 h\delta^2\frac{\xi+3R}{\xi-R}. \tag{5}$$

where A is the deformation area of the upper face sheet and ε_r the radial tensile strain, which can be approximately calculated by

$$\varepsilon_r=\frac{1}{2}\left(\frac{\partial w}{\partial r}\right)^2. \tag{6}$$

The plastic work due to compressive deformation of foam core is calculated by

$$D=\int_V\sigma_{\mathrm{pl}}\mathrm{d}V=\int_0^\xi\sigma_{\mathrm{pl}}w(r)\cdot 2\pi r\mathrm{d}r=\frac{\pi}{6}\sigma_{\mathrm{pl}}\delta(\xi^2+2R\xi+3R^2), \tag{7}$$

where V is the volume of the crushed foam. By summing up Eqs. 3, 5, and 7, the total potential energy is determined as

$$\prod=\frac{\pi}{3}\sigma_0 h\delta^2\frac{\xi+3R}{\xi-R}+\frac{\pi}{6}\sigma_{\mathrm{pl}}\delta(\xi^2+2R\xi+3R^2)-\int_0^\delta P\mathrm{d}\delta. \tag{8}$$

By minimizing π with respect to δ, the indentation force can be determined as

$$P=\frac{2\pi}{3}\sigma_0 h\delta\frac{\xi+3R}{\xi-R}+\frac{\pi}{6}\sigma_{\mathrm{pl}}(\xi^2+2R\xi+3R^2). \tag{9}$$

Besides the undetermined parameter ξ, the above expression includes two key material parameters (σ_0 and σ_{pl}) and two geometric parameters (h and R). A dimensionless parameter φ, defined by

$$\varphi=\frac{\sigma_{\mathrm{pl}}R}{\sigma_0 h}, \tag{10}$$

is introduced to examine the effect of material and geometric parameters on the indentation response. Some other dimensionless parameters are defined by

$$\overline{P}=\frac{P}{\sigma_0 Rh},\ \bar{\xi}=\frac{\xi}{R},\ \bar{\delta}=\frac{\delta}{R},\ \bar{h}=\frac{h}{R}. \tag{11}$$

Thereafter, the formulation of dimensionless indentation force can be rewritten as

$$\overline{P}=\frac{2\pi}{3}\bar{\delta}\frac{\bar{\xi}+3}{\bar{\xi}-1}+\frac{\pi}{6}\varphi(\bar{\xi}^2+2\bar{\xi}+3). \tag{12}$$

The principle of minimum work has been applied to determine the extent of deformation and indentation force [15]. It requires that the radius of deformation region $\bar{\xi}$ should satisfy the condition of the minimum force for a given indentation displacement, i.e. $\partial\overline{P}/\partial\bar{\xi}=0$. This results to a simple relationship between $\bar{\xi}$ and $\bar{\delta}$, i.e.

$$\bar{\delta}=\frac{\varphi}{8}(\bar{\xi}+1)(\bar{\xi}-1)^2. \tag{13}$$

By substituting Eq. (13) back into Eq. (12), the dimensionless indention force is determined as

$$\overline{P} = \frac{\pi\varphi}{12}(\bar{\xi}^3 + 5\bar{\xi}^2 + 3\bar{\xi} + 3). \tag{14}$$

From Eq. (13), we can determine the parameter of $\bar{\xi}$, i.e.

$$\bar{\xi} = \frac{1}{3} + \frac{2}{3}(\tilde{\delta}^{-1/3} + \tilde{\delta}^{1/3}), \tag{15}$$

where

$$\tilde{\delta} = -1 + \frac{27}{2}\frac{\bar{\delta}}{\varphi} + 9\sqrt{\left(\frac{3\bar{\delta}}{2\varphi}\right)^2 - \frac{1}{3}\frac{\bar{\delta}}{\varphi}}. \tag{16}$$

And then, the dimensionless indention force can be rewritten as

$$\overline{P} = \frac{\pi\varphi}{81}[67 + 36(\tilde{\delta}^{-1/3} + \tilde{\delta}^{1/3}) + 18(\tilde{\delta}^{-2/3} + \tilde{\delta}^{2/3}) + 2(\tilde{\delta}^{-1} + \tilde{\delta})]. \tag{17}$$

It should be noted that, if $\tilde{\delta} < 0$, we need to use $\tilde{\delta}^{\pm 1/3} = [(1 \pm i\sqrt{3})/2](-\tilde{\delta})^{\pm 1/3}$ and $\tilde{\delta}^{\pm 2/3} = [(-1 \pm i\sqrt{3})/2](-\tilde{\delta})^{\pm 2/3}$ with i being the imaginary unit. At the initial indention when $\bar{\delta} = 0$, we have $\tilde{\delta} = -1$, $\bar{\xi} = 1$ and $\overline{P} = \pi\varphi$, where the last relation corresponds to $P = \pi R^2\sigma_p$. This means that for a finite flat indenter, there is an initial indentation force.

2.2. Under a spherical indenter

The contact radius remains as the indenter radius for the indentation under a flat indenter, but for the indentation under a spherical indenter, the contact radius, a, may vary with indentation. The top face sheet within the contact region would conform to the spherical shape of the indenter. Generally, the contact radius is much smaller than the indenter radius R, and the displacement field of the top face sheet could be approximated by

$$w = \begin{cases} \delta - (R - \sqrt{R^2 - r^2}) \approx \delta - \frac{r^2}{2R}, & r \leqslant a \\ (\delta - \frac{a^2}{2R})\left(1 - \frac{r-a}{\xi - a}\right)^2, & a < r \leqslant \xi \end{cases} \tag{18}$$

Similar to the derivations in Section 2.1, the plastic strain energy of the top face sheet U is calculated as

$$U = \frac{\pi}{4}N_0\frac{a^4}{R^2} + \frac{\pi}{3}N_0\left(\delta - \frac{a^2}{2R}\right)^2\frac{\xi + 3a}{\xi - a} \tag{19}$$

and the plastic work due to compressive deformation of foam core D is given by

$$D = \frac{1}{6}\pi\sigma_{pl}\left[3\delta a^2 + \left(\delta - \frac{a^2}{2R}\right)(\xi^2 + 2a\xi)\right]. \tag{20}$$

Thereafter, the dimensionless indenter force can be determined as

$$\overline{P} = \frac{2\pi}{3}\left(\bar{\delta} - \frac{1}{2}\bar{a}^2\right)\frac{\bar{\xi} + 3\bar{a}}{\bar{\xi} - \bar{a}} + \frac{\pi}{6}\varphi(\bar{\xi}^2 + 2\bar{a}\bar{\xi} + 3\bar{a}^2) \tag{21}$$

where $\bar{a} = a/R$. There are two unknown parameters ($\bar{\xi}$ and $\bar{a}$) in the above expression. Using the condition that partial derivatives of indentation force with respect to the two unknown parameters equals zero, we have

$$\begin{cases} (\bar{\delta} - \frac{1}{2}\bar{a}^2)\bar{a} - \frac{1}{8}\varphi(\bar{\xi} + \bar{a})(\bar{\xi} - \bar{a})^2 = 0 \\ 2\bar{a}^2(\bar{\xi} + 3\bar{a}) - \varphi(\bar{\xi} - \bar{a})(\bar{\xi}^2 + 2\bar{\xi}\bar{a} + 3\bar{a}^2) = 0 \end{cases} \tag{22}$$

Here, we introduce two parameters, u and v, defined by

$$u = \bar{\xi}/\bar{a} \quad \text{and} \quad v = \bar{\delta}/\bar{a}^2, \tag{23}$$

respectively. Thus, Eq. (22) can be transformed to

$$\begin{cases} \frac{2(u+3)}{(u-1)(u^2+2u+3)} = \varphi \\ v = \frac{1}{2} + \frac{1}{8}\varphi(u+1)(u-1)^2 \end{cases} \tag{24}$$

The above relations show that the two parameters, u and v, depend on the only parameter φ. Solving the first relation with $\varphi > 0$, we have a positive solution

$$u = \frac{1}{3}[-1 + 2(3 - \varphi)\psi^{-1/3} + \varphi^{-1}\psi^{1/3}]$$

with

$$\psi = 72\varphi^2 + 44\varphi^3 - 6\sqrt{6}(-\varphi^3 + 25\varphi^4 + 29\varphi^5 + 9\varphi^6)^{1/2}.$$

The dimensionless indentation force can be simplified as

$$\overline{P} = \frac{\pi}{3}\varphi(u^2 + 2u + 3)\bar{\delta}. \tag{25}$$

It is interesting that the indenter load increases linearly with the increase of the displacement and its slope is only relative to the dimensionless parameter φ. In fact, the dimensionless parameter φ is a small parameter, so we can obtain asymptotic solutions for the parameters u and v

$$\begin{cases} u = \frac{2}{\sqrt{2\varphi}} + \frac{3}{5} + O(\sqrt{\varphi}) \\ v = \frac{1}{2\sqrt{2\varphi}} + \frac{7}{10} + O(\sqrt{\varphi}) \end{cases}, \tag{26}$$

and for the parameters $\bar{a}$, $\bar{\xi}$ and $\overline{P}$

$$\bar{a} = \sqrt{\bar{\delta}/v} = 2^{3/4}\varphi^{1/4}\left(1 - \frac{7}{10}\sqrt{2\varphi} + O(\varphi)\right)\bar{\delta}^{1/2}, \tag{27}$$

$$\bar{\xi} = u\sqrt{\bar{\delta}/v} = 2^{5/4}\varphi^{-1/4}\left(1 - \frac{2}{5}\sqrt{2\varphi} + O(\varphi)\right)\bar{\delta}^{1/2}, \tag{28}$$

$$\overline{P} = \frac{2\pi}{3}\left(1 + \frac{8}{5}\sqrt{2\varphi} + O(\varphi)\right)\bar{\delta}. \tag{29}$$

Eqs. (27) and (28) show that $\bar{a}$ and $\bar{\xi}$ are proportional to the square root of $\bar{\delta}$, but the proportionality coefficients are in the order of $O(\varphi^{1/4})$ and $O(\varphi^{-1/4})$, respectively.

In the analytical modeling, the parabolic approximation of the shape of the spherical indenter used is valid when the contact radius, a, is much less than the indenter radius, R, i.e. $\bar{a} \ll 1$. From Eq. (27), the analytical solutions is valid when the indentation displacement satisfy

$$\bar{\delta} \ll 2^{-3/2}\varphi^{-1/2}. \tag{30}$$

Since the parameter φ is a small parameter, the parabolic approximation is valid for a deep indentation. For example, the analytical solutions may be applied until the dimensionless indentation displacement is no longer much smaller than 1.58 when $\varphi = 0.05$.

3. Numerical modeling

The numerical modeling was performed by using the ABAQUS/Explicit finite element code. The indenter was modeled as a rigid body. The foam core and the face sheets were simulated using 8-node linear brick (C3D8R) finite elements and four-node shell elements (S4R) with reduced integration, respectively. The finite element mesh of the sandwich structures was condensed towards center of circular panels. The contact with no separation between the face sheet and foam core was modeled through the TIE interaction. The indenter has a constant vertical velocity of 1 m/s, and the lower and edge boundary of the sandwich circular panels were fully clamped. Recent experimental study has revealed that indentation force–displacement relations for quasi-static indentation and low-velocity impact are virtually equivalent [16,17], so a large velocity of the indenter was selected to decrease the computing time.

Table 1
Simulation cases to verify the analytical solutions.

ρ_f/ρ_s	σ_{pl} (MPa)	σ_0 (MPa)	h (mm)	R (mm)	φ
0.05	1.245	602.5	2	5	0.0052
0.1	3.523	602.5	2	5	0.0146
0.1	3.523	602.5	2	10	0.0292
0.1	3.523	602.5	1	10	0.0584

The mechanical properties of face sheet material were taken from Ref. [18] for stainless steel Cr18Ni8. Mechanical properties of metallic foams can be described by those of its matrix material and relative density, which is defined by the ratio of the density of foam ρ_f to that of its matrix material ρ_s. More details can be referred to our previous study [14] and relative literature [19,20]. In the numerical models, the crushable foam model with volumetric hardening was used to model the foam material.

The effects of the radius of sandwich circular panels, R_0, and the thickness of foam cores, h, are ignored in the analytical models. In the numerical models, we choose $R_0 = 100$ mm and $h = 25$ mm to ensure a reasonable degree of approximations.

From the analytical results, it can be found that the key factor, which determines the deformation and load-carry capacity of indentation response, is the combined parameter φ rather than the separate four ones, i.e. σ_0, σ_{pl}, h and R. Hence, four cases for φ are chosen in this paper, as listed in Table 1.

4. Results and discussion

4.1. The profiles of the deformation zone

The form of the displacement field of the dented zone is the key of theoretical modeling, which directly determines its operability and validity. Its validity could be verified by comparing the profiles of the deformation zone from theoretical model with those from simulations.

The results for the case of flat indenter with $\varphi = 0.0292$ are shown in Fig. 2a. It can be found that, the predicted profiles are in close agreement with those from simulation outside of the indenter. However, the part of face sheet under the flat indenter separates from indenter in the denting process, which was not considered in the analytical model. In fact, the edge of the contact region cannot rotate freely due to flexible rigidity of the face sheet, which leads to appearance of a dent under the indenter.

Under a spherical indenter, a similarly close agreement is demonstrated, see Fig. 2b, however the radius of the deformation zone has a small difference. In analyzing an infinite, orthotropic, elastic plate on a rigid-plastic foundation under a hemispherical-nose indenter, Turk et al. [9] used a constant effective radius, $0.4R$, to approximate the contact radius in terms of experimental results of other researcher [21], but Eq. (27) in the present model indicates that the contact radius increases linearly with indenter displacement.

4.2. The distribution of the stretching strain of the face sheets

Substituting Eqs. (4) into (6), we obtain the plastic tensile strain of the top face sheet dented by a flat cylinder

$$\varepsilon_r = \frac{2\delta^2}{(\xi - R)^2}\left(1 - \frac{r-R}{\xi - R}\right)^2, R < r \leqslant \xi \tag{31}$$

which shows that the plastic strain demonstrates the same distribution law as the displacement outside of the indenter. The maximum strain arises at radius $r = R$. When the indenter is of spherical shape, the maximum value appears at the edge of contact region instead.

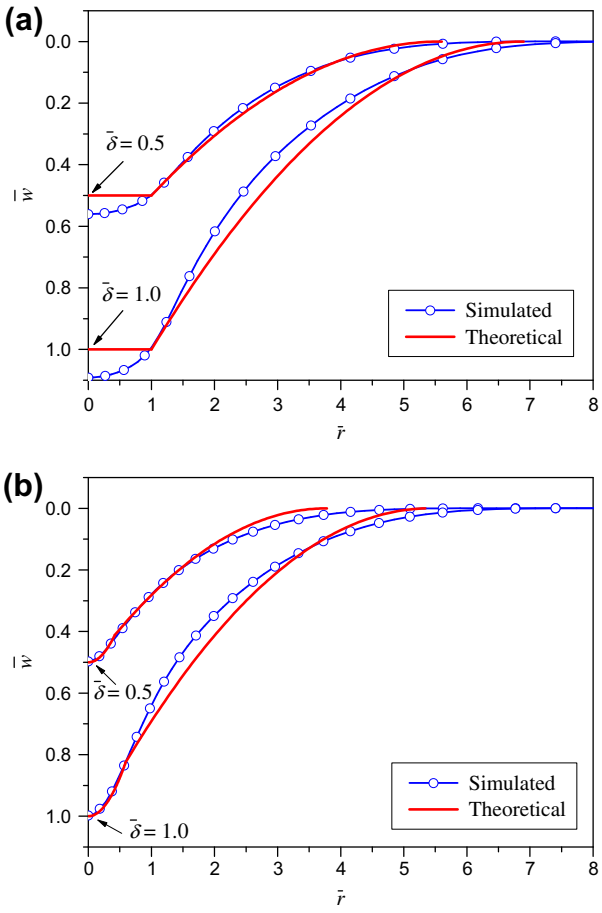

Fig. 2. Distributions of face sheet deformation for $\varphi = 0.0292$: (a) under a flat indenter and (b) under a spherical indenter.

Of course, while the maximum strain achieves the ultimate fracture strain of upper face sheet material, the upper face sheet would rupture and fail. Our attention is mostly paid to the structural response, and the material rupture effect was not considered in the models.

4.3. Indentation force

It can be found that the dimensionless indentation force of the flat indenter has an initial value $\pi\varphi$ when the indenter displacement is zero, as mentioned above. This initial value is due to compressive deformation of foam core just under the indenter, which would remain constant during denting. Since φ is a small parameter, this initial value does not seem obvious in Fig. 3a. Fig. 3a shows that for the case $\varphi = 0.0052$, there is some difference between the predicted load and the simulated result, but with φ increasing, they go very close to each other.

When the indenter is of the sphere shape, the indentation force increases linearly with the indenter displacement, see Eq. (25), and this linear function can be rewritten in a unified form, as shown in Fig. 3b. However, the numerical results display an initial non-linear stage, which is caused by the elastic property in the numerical models. Additionally, for very small φ such as 0.0052 or 0.0146, the theoretical models are not so close to the numerical results, but this situation is changed when φ increases.

4.4. Characteristics of energy absorption

It is well-known that the total internal energy absorption comprises of two parts: energy dissipated by plastic deformation and

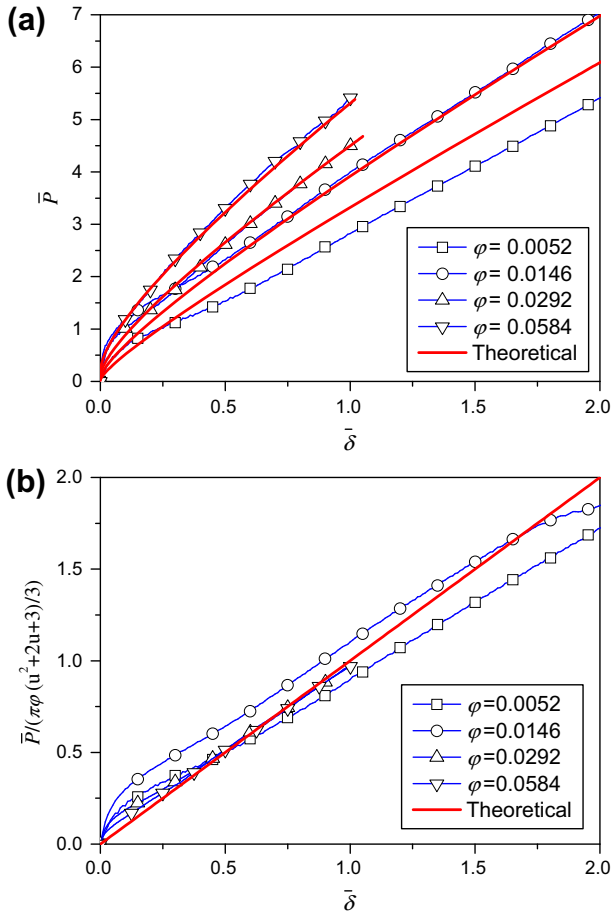

Fig. 3. Indentation force–displacement curves: (a) under a flat indenter and (b) under a spherical indenter.

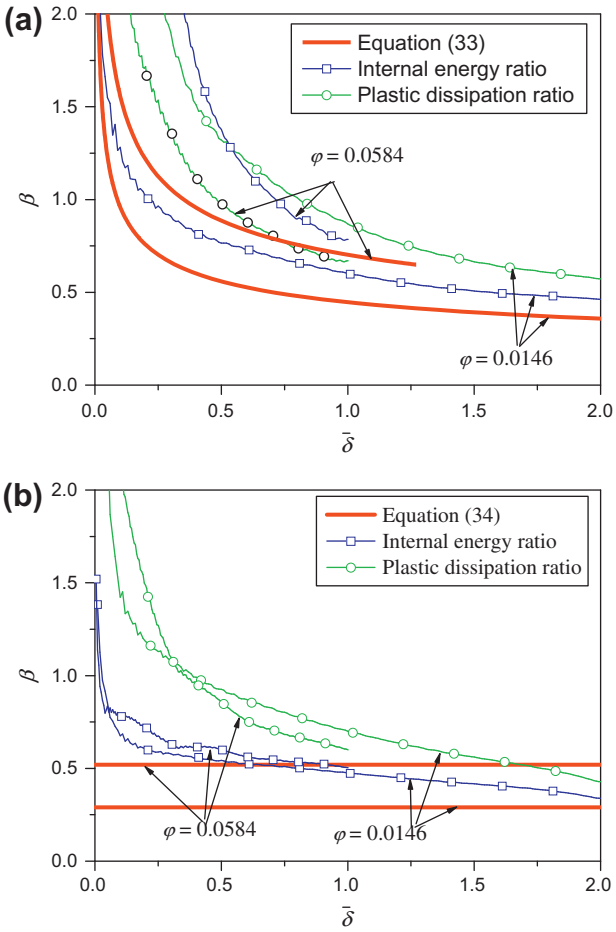

Fig. 5. Ratio of energy dissipation of foam core to that of the upper face sheet: (a) under a flat indenter and (b) under a spherical indenter.

recoverable strain energy from elastic deformation. The latter was not considered in the present analytical solutions, but the numerical results can reveal its effect. For facility, we define a parameter α as

$$\alpha = \frac{\text{Plastic dissipation}}{\text{Internal energy}}. \tag{32}$$

Obviously, when the value of α comes closer to 1, plastic dissipation approaches more to internal energy and elastic strain energy could be neglected. The development of α with indenter displacement for the case $\varphi = 0.0292$ was shown in Fig. 4, and other cases display the similar characteristic. It can be found that plastic dissipation approaches to internal energy with indenter displacement increasing. The foam core is dominated by plastic deformation after a short displacement due to its low rigidity and yield stress.

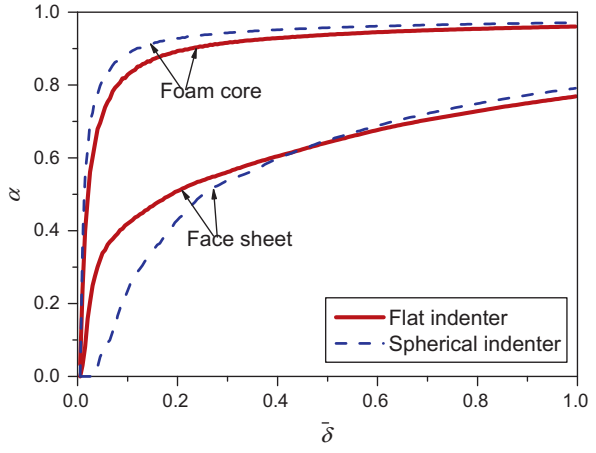

Fig. 4. Energy absorption characteristic from FE simulation for the case $\varphi = 0.0292$.

Using the analytical solutions, we can calculate the ratio of energy dissipation due to the compressive deformation of foam to that due to the radial membrane deformation of the upper face sheet. This ratio for the case of a flat indenter is

$$\beta = \frac{D}{U} = \frac{4(\bar{\xi}^2 + 2\bar{\xi} + 3)}{(\bar{\xi}^2 - 1)(\xi + 3)}, \tag{33}$$

and that of a spherical indenter is

$$\beta = 2\varphi \frac{3v + (v - \frac{1}{2})(u^2 + 2u)}{3 + 4(v - \frac{1}{2})^2 \frac{u+3}{u-1}} \sim 2\sqrt{2\varphi}(1 - \sqrt{2\varphi} + O(\varphi)). \tag{34}$$

Under a flat indenter, the ratio of energy absorption decreases with increasing displacement and increases with increasing φ, see Fig. 5a. When the displacement is small, $\alpha > 1$, in other words, the energy absorption mostly derives from the compressive deformation of the foam core, whereafter contribution of face sheet would become larger and larger. Under a spherical indenter, the ratio keeps constant in the denting process, but increases with increasing φ likewise, as shown in Fig. 5b. The plastic dissipation ratio of foam core to that of face sheet has much discrepancy from analytical solutions, either under flat indenter or under spherical one, while

internal energy ratio comes closer to them. This discrepancy may be mostly caused by elastic strain energy outside the deformed zone, which was not considered in the analytical models. When elastic strain energy is small, plastic dissipation ratio may approaches to internal energy one and analytical solutions.

5. Conclusions

Local indentation response of sandwich circular panels on a rigid base is analyzed based on the principle of minimum potential energy. In the analytical models, elastic response of the composite structure was neglected, and the upper face sheet was modeled as an infinite, ideally plastic thin plate resting on a rigid-plastic foundation, which gives a constant crushing resistance by the foam core. A quadratic polynomial displacement field was proposed to describe the deformation of the top face sheet. An FEA model was established using the ABAQUS code to verify the validity and applicability of the analytical solutions. In terms of the analytical solutions, distribution of radial tensile strain of the upper face sheet and the ratio of energy dissipation of foam core to that of the upper face sheet were analyzed.

Acknowledgements

This work is supported by the National Natural Science Foundation of China (Projects Nos. 90916026, 10532020 and 10672156) and the Chinese Academy of Sciences (Grant No. KJCX2-EW-L03).

References

[1] Rizov V, Shipsha A, Zenkert D. Indentation study of foam core sandwich composite panels. Compos Struct 2005;69:95–102.
[2] Rizov V, Mladensky A. Influence of the foam core material on the indentation behavior of sandwich composite panels. Cell Polym 2007;26:117–31.
[3] Rizov V. Indentation of foam-based polymer composite sandwich beams and panels under static loading. J Mater Eng Perform 2009;18:351–60.
[4] Mohan K, Yip TH, Sridhar I, Seow HP. Effect of face sheet material on the indentation response of metallic foams. J Mater Sci Technol 2007;42:3714–23.
[5] Anderson T, Madenci E. Graphite/epoxy foam sandwich panels under quasi-static indentation. Eng Fract Mech 2000;67:329–44.
[6] Anderson TA. A 3-D elasticity solution for a sandwich composite with functionally graded core subjected to transverse loading by a rigid sphere. Compos Struct 2003;60:265–74.
[7] Koissin V, Skvortsov V, Krahmalev S, Shilpsha A. The elastic response of sandwich structures to local loading. Compos Struct 2004;63:375–85.
[8] Du L, Jiao GQ. Indentation study of Z-pin reinforced polymer foam core sandwich structures. Compos Part A – Appl Sci 2009;40:822–9.
[9] Turk MH, Fatt MSH. Localized damage response of composite sandwich plates. Compos Part B – Eng 1999;30:157–65.
[10] Koissin V, Shipsha A, Rizov V. The inelastic quasi-static response of sandwich structures to local loading. Compos Struct 2004;64:129–38.
[11] Griffith J, Vanzant H. Large deformation of circular membranes under static and dynamic loads. In: Proceedings of the first international congress on experimental mechanics. New York; November, 1961. p. 99–109.
[12] Jones N. Structural impact. Cambridge: Cambridge University Press; 1989.
[13] Zaera R, Arias A, Navarro C. Analytical modelling of metallic circular plates subjected to impulsive loads. Int J Solids Struct 2002;39:659–72.
[14] Xie ZY, Zheng ZJ, Yu JL. Localized indentation of sandwich beam with metallic foam core. J Sandw Struct Mater 2012;14(2):197–210.
[15] Soden PD. Indentation of composite sandwich beams. J Strain Anal Eng 1996;31:353–60.
[16] Ferri R, Sankar BV. Static indentation and low velocity impact tests on sandwich plates. In: Proceeding of the 1997 ASME international mechanical engineering congress and exposition, Dallas, TX, USA; 1997. p. 485–90.
[17] Lindholm CJ. Impact and indentation behavior of sandwich panels – modeling and experimental testing. Sandw Struct 7: Advance Sandw Struct Mater 2005:635–42.
[18] Santosa S, Banhart J, Wierzbicki T. Experimental and numerical analyses of bending of foam-filled sections. Acta Mech 2001;148:199–213.
[19] Gibson LJ, Ashby MF. Cellular solids: structure and properties. Cambridge: Cambridge University Press; 1997.
[20] Santosa S, Wierzbicki T. On the modeling of crush behavior of a closed-cell aluminum foam structure. J Mech Phys of Solids 1998;46:645–69.
[21] Williamson JE, Lagace PA. Response mechanisms in the impact of graphite/epoxy honeycomb sandwich panels. In: The proceedings of the eight technical conference of the American society for composites. Ohio: Cleveland; 1993. p. 287–97.